Phase advance and β function measurements using model-independent analysis

Chun-xi Wang,* Vadim Sajaev, and Chih-Yuan Yao
Argonne National Laboratory, 9700 South Cass Avenue, Argonne, Illinois 60439, USA
(Received 20 December 2002; published 22 October 2003)

Phase advance and β function are basic lattice functions characterizing the linear properties of an accelerator lattice. Accurate and efficient measurements of these quantities are important for commissioning and operating a machine. For rings with little coupling, we report a new method to measure these lattice functions based on the model-independent analysis technique, which uses beam histories of excited betatron oscillations measured simultaneously at a large number of beam position monitors. It is simple, fast, accurate, and robust. Measurements done at the storage ring of the Advanced Photon Source are reported. Comparisons among various methods are made.

DOI: 10.1103/PhysRevSTAB.6.104001 PACS numbers: 41.85.–p

I. INTRODUCTION

Beam orbits in an accelerator are usually dominated by the linear properties of its lattice. In most lattices, coupling between the two transverse degrees of freedom is kept at a minimum. In this paper we will ignore transverse coupling. To a good approximation, a transverse orbit can usually be described by

$$x(s) = x_0(s) + x_\beta(s) + D_x(s)\delta, \tag{1}$$

where x_0 is the zeroth order orbit around which occur small betatron oscillations x_β and oscillations coupled from the energy δ oscillation through the dispersion D_x. Here x represents either horizontal or vertical beam positions. The betatron oscillation can be described by the well-known expression

$$x_\beta(s) = \sqrt{2J\beta(s)}\cos[\phi + \psi(s)], \tag{2}$$

where $\{J, \phi\}$ are the action-angle variables specifying a specific orbit, $\beta(s)$ is the beta function, and $\psi(s)$ is the phase advance. The lattice functions β and ψ as well as D_x characterize the linear properties of a lattice. It is an important and routine task to measure these lattice functions. The transverse orbit information is primarily collected from a large number of beam position monitors (BPMs) along a machine. Many methods have been developed to derive the lattice functions from BPM measurements [1,2] . Some depend on narrow-band BPMs that can measure only the closed orbits; others use broad-band BPMs capable of measuring beam histories on a turn-by-turn basis.

The most basic techniques to measure β function are based on varying a quadrupole or a dipole corrector and deducing the β function at the magnets from corresponding tune or closed-orbit changes, respectively. These techniques are simple but slow (especially when a large number of magnets are used) and require independently powered magnets with reliable calibration. A fast technique based on orbit oscillations measured with broadband BPMs was developed and successfully used to measure the phase advances in LEP (Large Electron Position Collider at CERN) [3,4]. It determines the betatron phase at each BPM by computing the sine and cosine coefficients of a resonantly excited harmonic betatron oscillation. A similar technique was implemented in the Cornell Electron/Position Storage Ring, where a signal analyzer effectively accomplished the harmonic analysis [5].

The above methods measure the phase advance and β function directly. There are two methods that fit a machine model with measurements, and the phase advance and beta function are by-products of the fitted model. One of them is the response-matrix method that has been successfully used on many machines [6–10]. The basic idea is to minimize the difference between measured and calculated (from a model) BPM responses to changes in steering magnet strengths by adjusting various model parameters such as corrector strengths, quadrupole gradients, and BPM gains. The other one is a new method developed for PEP-II at SLAC [11–13]. It extracts four high-quality linearly independent betatron orbits from simultaneously acquired beam histories at all broadband BPMs, then computes the Green's function elements of the transfer matrices between BPMs and fits them with a model. An obvious advantage of using beam histories is that it takes a much shorter time to acquire the data. If there is a sufficient number of BPMs and a good model is available, the model-fitting methods provide systematic and powerful tools to calibrate model parameters.

In recent years, model-independent analysis (MIA) emerged as a new approach to study beam dynamics by analyzing simultaneously recorded beam histories at a large number of BPMs [14,15]. A basic technique used in MIA is the spatial-temporal mode analysis via a singular value decomposition (SVD) of the data matrix containing beam histories. Similar to the Fourier analysis, SVD mode analysis decomposes the spatial-temporal variation of the beam centroid into superposition of various

*Electronic address: wangcx@aps.anl.gov

orthogonal modes by effectively accomplishing a major statistical data analysis, namely, the principal component analysis [16,17]. Let b_p^m represent the measurement at the mth monitor for the pth pulse or turn. Then the singular value decomposition of the beam-history matrix $B_{P\times M} = (b_p^m)$ gives

$$B = USV^T = \sum_{\text{modes}} \sigma_i u_i v_i^T, \tag{3}$$

where $U_{P\times P} = [u_1, \cdots, u_P]$ and $V_{M\times M} = [v_1, \cdots, v_M]$ are orthonormal matrices comprising the temporal and spatial eigenvectors, and $S_{P\times M}$ is a rectangular matrix with non-negative singular values σ_i along the upper diagonal. A pair of spatial and temporal vectors characterizes an eigenmode and the corresponding singular value specifies the overall amplitude of the eigenmode. In this paper, we will show that when beam motion is dominated by betatron oscillations, there are two orthogonal eigenmodes corresponding to the normal coordinates that are normally used to describe the betatron motion. From these two betatron modes, the phase advance and beta function can be derived with good accuracy.

In the following, we first describe the simple theory of our technique by showing that the SVD eigenmodes yield the betatron modes, from which the lattice functions are derived. Then we report experiments done at the storage ring of the Advanced Photon Source (APS). Based on our experience, we compare our technique with commonly used ones and argue certain advantages of our technique.

II. MIA TECHNIQUE TO MEASURE LATTICE FUNCTIONS

A. Betatron modes

Since BPMs measure beam centroid motion, the beam histories recorded by the BPMs may be quite different from single-particle motion, even though individual particles can be described by Eq. (2). To accommodate this fact, we assume the mth BPM reading for the pth pulse can be expressed in action-angle variables $\{J_p, \phi_p\}$ as

$$b_p^m = \sqrt{2J_p\beta_m}\cos(\phi_p + \psi_m), \tag{4}$$

where β_m is the β function at the mth BPM, and ψ_m is the phase advance from a starting point to the mth BPM. For simplicity, BPM noise is ignored here. Note that a subscript p is given to the action and angle variables. In a linac, this accounts for the different initial conditions of each pulse. In a ring, it accommodates action and angle variations from turn to turn. For an ideal linear system, the action is conserved and the angle simply advances by the tune each turn. However, nonlinear effects and damping of the beam centroid can lead to much more complicated action-angle variation although they do not deviate much from single-particle behavior within each turn.

Now let us compute the eigenmodes analytically. For convenience, we use $B = (b_p^m)/\sqrt{P}$ so that the variance-covariance matrix is simply given by $C_B = B^T B$. From the BPM data given by Eq. (4), the elements of C_B read

$$\begin{aligned}(C_B)_{mn} &= \frac{1}{P}\sum_{p=1}^{P} b_p^m b_p^n \\ &= \sum_{p=1}^{P}\frac{J_p}{P}\sqrt{\beta_m\beta_n}[\cos(\psi_m-\psi_n)+\cos(2\phi_p+\psi_m+\psi_n)] \\ &= \langle J\rangle_p\sqrt{\beta_m\beta_n}\cos(\psi_m-\psi_n),\end{aligned} \tag{5}$$

where $\langle J\rangle_p$ is the ensemble average of the action. The subscript p is dropped hereafter. The last term involving ϕ_p averages to zero for sufficiently large P, provided that the action and angle are independently distributed. From Eq. (3),

$$C_B V = (USV^T)^T(USV^T)V = VS^2, \tag{6}$$

thus, the spatial vectors of B are the eigenvectors of C_B and the singular values are the square roots of the eigenvalues of C_B, i.e., $\sigma = \sqrt{\lambda}$.

To find the eigenvalues and eigenvectors of C_B, we need to solve the secular equation

$$C_B v = \lambda v. \tag{7}$$

Since the B matrix is formed by a set of linear betatron orbits, the eigenvector v must be a betatron orbit as well, i.e., v is of the form $v = \{\sqrt{2J\beta_m}\cos(\phi_0 + \psi_m), m = 1, \ldots, M\}$ where ϕ_0 and J are to be determined by the secular equation and normalization of v, respectively.

From the mth component of the secular equation,

$$\begin{aligned}\lambda\cos(\phi_0+\psi_m) &= \langle J\rangle\sum_{n=1}^{M}\beta_n\cos(\psi_m-\psi_n)\cos(\phi_0+\psi_n) \\ &= \langle J\rangle\Bigg[\cos(\phi_0+\psi_m)\sum_{n=1}^{M}\beta_n\cos^2(\phi_0+\psi_n) \\ &\quad +\frac{1}{2}\sin(\phi_0+\psi_m)\sum_{n=1}^{M}\beta_n\sin 2(\phi_0+\psi_n)\Bigg].\end{aligned} \tag{8}$$

Therefore, we have the condition

$$\sum_{n=1}^{M}\beta_n\sin 2(\phi_0 + \psi_n) = 0. \tag{9}$$

There are two solutions,

$$\phi_0 = -\frac{1}{2}\arctan\left(\frac{\sum_n \beta_n \sin 2\psi_n}{\sum_n \beta_n \cos 2\psi_n}\right) \tag{10}$$

and $\phi_0 + \frac{\pi}{2}$, that lead to two different eigenvectors. The two eigenvalues are

$$\lambda_{\pm} = \frac{1}{2}\langle J\rangle\left[\sum_{n=1}^{M}\beta_n + \sum_{n=1}^{M}\beta_n \cos 2(\phi_0+\psi_n)\right] = \frac{1}{2}\langle J\rangle\left[\sum_{n=1}^{M}\beta_n \pm \sqrt{\left(\sum_n \beta_n \cos 2\psi_n\right)^2 + \left(\sum_n \beta_n \sin 2\psi_n\right)^2}\right]. \tag{11}$$

Note that the leading term is proportional to $M\langle J\rangle_p\langle\beta\rangle_m$ that grows with the number of BPMs used. (It is often convenient to remove such dependence when using singular values by normalizing the data matrix.) The normalized eigenvectors are

$$\begin{cases} v_+ = \frac{1}{\sqrt{\lambda_+}}\{\sqrt{\langle J\rangle\beta_m}\cos(\phi_0+\psi_m),\ m=1,\ldots,M\}, \\ v_- = \frac{1}{\sqrt{\lambda_-}}\{\sqrt{\langle J\rangle\beta_m}\sin(\phi_0+\psi_m),\ m=1,\ldots,M\}. \end{cases} \tag{12}$$

These two vectors are obviously orthogonal according to Eq. (9). Note that these betatron vectors are independent single-particle betatron trajectories even though the centroid motion is not. The normalized temporal vectors that are consistent with the spatial vectors are

$$\begin{cases} u_+ = \{\sqrt{\frac{2J_p}{P\langle J\rangle}}\cos(\phi_p-\phi_0),\ p=1,\ldots,P\}, \\ u_- = \{-\sqrt{\frac{2J_p}{P\langle J\rangle}}\sin(\phi_p-\phi_0),\ p=1,\ldots,P\}, \end{cases} \tag{13}$$

which clearly relate to the commonly used normal coordinates. Note that the orthogonality of these two vectors holds for $P\to\infty$. In other words, for finite P, these expressions are only approximate. So is Eq. (5).

Summarizing the above eigenanalysis, the SVD of the beam-history matrix of the betatron oscillation (without noise, otherwise more terms are needed) is given by

$$B \equiv \frac{1}{\sqrt{P}}(b_p^m) = \sigma_+ u_+ v_+^T + \sigma_- u_- v_-^T, \tag{14}$$

where the singular values $\sigma_\pm = \sqrt{\lambda_\pm}$, and the spatial and temporal singular vectors are the column vectors given by Eqs. (12) and (13). Remarkably, the spatial and temporal vectors yield independent single-particle betatron motion and the well-known normal coordinates for this 1D dynamical system. There are only two terms in the above decomposition because the betatron motion is in two dimensional phase space. Note that there is a sign ambiguity in the singular vectors. By definition the singular values are non-negative and the singular vectors are normalized to one. But for a pair of singular vectors u and v, their negatives, $-u$ and $-v$, can also be chosen as the singular vectors.

In practice the measured beam histories contain not only the dominating betatron oscillation but also BPM noises as well as motions due to other small perturbations. It is difficult to analytically study the eigenmodes for more complicated systems. Nonetheless, there is a matrix theorem that states that $O(\epsilon)$ changes in B can alter a singular subspace by an amount ϵ/Δ, where Δ measures the separation of the relevant singular values [18]. Thus, as long as the singular values of the betatron modes are far from the rest, Eq. (14) should be a good representation of the measured betatron modes.

B. Determination of phase advance and β function

From the betatron vectors, Eq. (12), the phase advances can be determined as

$$\psi = \tan^{-1}\left(\frac{\sigma_- v_-}{\sigma_+ v_+}\right), \tag{15}$$

where the phase ϕ_0 is absorbed by shifting the reference point of the phase. Since we are interested in only the phase advance between BPMs, the reference point does not matter. The β function can be written as

$$\beta = \langle J\rangle^{-1}(\lambda_+ v_+^2 + \lambda_- v_-^2). \tag{16}$$

Note that, except for an overall scaling factor $\langle J\rangle$ in β, the phase advance and β function can be computed from the betatron vectors obtained by an SVD analysis of the beam-history matrix.

One complication in determining phase advances with Eq. (15) is the uncertainty due to the inverse trigonometric function and the sign ambiguity of the betatron vectors. Fortunately, the local phase-advance deviations from a machine model are generally much less than π; therefore, with estimated phase advances from even a crude machine model, the phase uncertainty can be resolved. Furthermore, it is not difficult to see that errors in BPM gains have no effect on the phase-advance measurement since they will be canceled in Eq. (15). In short, from the betatron vectors, the phase advances between BPMs can be uniquely determined, and the technique is model independent and robust against BPM calibration errors.

It is difficult to obtain accurate error bounds for the measurements. However, the absolute errors in phase (in unit radian) and relative errors in β function can be estimated by (see Appendix A)

$$\sigma_\psi \simeq \frac{1}{\sqrt{P}}\frac{\sigma_r}{\sigma_s} \quad \text{and} \quad \sigma_{\Delta\beta/\beta} \simeq 2\sigma_\psi, \tag{17}$$

where σ_s is the rms strength of the betatron signal as measured by the singular values, and σ_r is the residual signal and noise that can be estimated by the quadratic sum of the singular values of nonbetatron signals and random noise. For pure harmonic oscillations with random BPM noise, σ_r is BPM resolution and $\sigma_s = A/\sqrt{2}$, where A is the oscillation amplitude; then Eq. (17) is the same as errors quoted for the harmonic analysis [4]. The apparent P dependence loses its power quickly for a pulse signal, whose singular value decreases with $\sqrt{P}$ for large P. For sufficiently large P, the random noise becomes a secondary contribution to the error, and the $\sqrt{P}$ dependence will not hold any more. σ_r is difficult

to estimate. Often the third largest singular value gives a rough estimate.

It is instructive to see the connection between the method developed here and the method based on harmonic analysis of orbit oscillations [4]. For a perfect linear system without noise, the temporal vectors are pure harmonics and the spatial vectors are simply the coefficients of these harmonics. Thus, the two methods for phase-advance measurement are basically the same, although one uses harmonic analysis to extract the sine and cosine coefficients of the betatron oscillation, and the other uses SVD to obtain the sine and cosine betatron orbits in Eq. (12). However, the two methods are fundamentally different. The harmonic analysis relies on the temporal signal having a constant amplitude and periodic phase in Eqs. (4) and (13) while the new method does not rely on the temporal vectors at all. Therefore, the new method is more robust in terms of tolerating all sorts of beam excitations as shown below and has wider applicability in the sense that it can be used under conditions not suitable for harmonic analysis.

Computing β function with Eq. (16), rather than simply using the amplitude of individual BPMs, has the advantage that the extracted betatron modes are cleaner since nonbetatron motion and noise have been excluded via mode analysis. However, one obvious limitation is that it depends on BPM gain calibration. Unfortunately, there is no simple way around this except fitting with machine models.

III. MEASUREMENTS DONE AT THE APS

To test the new method, experiments have been done at the APS storage ring using beam-history measurements at 360 broad-band BPMs with various kinds of beam excitations. Comparisons with the response-matrix and harmonic-analysis methods have been made. Good agreements were reached.

A. Obtaining the betatron modes

With reliable measurements of beam histories, it is straightforward to extract the betatron modes as in Eq. (14) via SVD mode analysis. Unfortunately, the beam-history modules of the current BPM system at the APS have various problems [19]. We will not discuss the details of confronting these problems with MIA. After identifying and removing the malfunctioning and noisy BPMs, about 3/4 of the 360 BPMs were used for the phase-advance and β function measurements. Another major obstacle is that these beam histories are not synchronized to the same turn. There is uncertainty about a couple of turns. It turns out that phase-advance measurement is an effective technique to detect the synchronization problem. For each turn offset at a BPM, the phase advance is changed according to the tune. In order to avoid integer and half-integer resonances, the fractional tune is usually much larger than the phase errors of the optics. Thus, by comparing the measured and designed phase advances, we are able to detect the out-of-sync beam histories and synchronize them by simply shifting the histories relative to each other (works for turn-by-turn but not for every-other-turn histories). The measured beam histories are further corrected with BPM gains obtained with the response-matrix method [10], which is necessary for the β function measurement. After the beam histories are cleaned, gain corrected, and synchronized, a final SVD mode analysis is performed to extract the betatron modes—the first two eigenmodes that dominate the beam motion. Fourier analysis of the temporal patterns of the betatron modes is performed to confirm that the betatron modes are well separated from other modes due to synchrotron oscillation, transverse coupling, nonlinear effects in optics and BPMs, and so on. Here we will not report the details of all the modes we observed, although they are very informative [20].

B. Horizontal measurements with kick excitation

For the horizontal plane, an injection kicker is used to kick a stored bunch to a desired amplitude, and the resulting betatron oscillation is recorded. Mode analysis yields about ten modes above the noise floor: the two largest modes are the betatron modes, the third one is the synchrotron mode due to residual energy oscillation in the ring, and so on. As examples, the first and the third modes are shown in Figs. 1 and 2. The second betatron mode is similar to the first one.

In Fig. 1, the spatial vector of the betatron mode is a betatron orbit. Because of the unusable BPMs (shown as red dots), the orbit is broken into pieces and looks irregular. The temporal vector clearly shows a beam that is kicked at about the 100th turn, then decohered and damped. By construct, both spatial and temporal vectors are normalized to one. The mode number and its singular value (in a unit of BPM count that is about 7 μm) are shown on the left-hand-side label. The Fourier spectrum of the temporal vector shows the betatron frequency with a broadened peak due to decoherence. Note that the synchrotron and vertical tunes as well as other nonlinear resonance frequencies are invisible, even though they do exist and show up in other modes [20]. This confirms the quality of the betatron modes. In Fig. 2, the spatial vector of the synchrotron mode (the third largest mode) corresponds to the dispersion. Again, the unusable BPMs broke the regular pattern. The temporal vector yields the residual energy oscillation in the ring, which is barely perturbed by the kick. The corresponding spectrum contains a clear synchrotron tune and various harmonics of the power line frequency.

The synchrotron mode and the noise floor are determined by the machine condition and BPM system, but independent of the kick strength. Increasing the kick

strength improves the signal-to-noise ratio. However, due to decoherence, the oscillation is significantly damped in tens of turns, and the larger the kick amplitude the quicker it damps; thus the overall signal strength is limited.

Using the spatial vectors of the two betatron modes and the procedure described in the last section, we obtained the phase advances and β function for the horizontal plane as shown in Fig. 3. MIA measurement results are shown as solid dots. For comparison, corresponding model values are shown as diamonds. Instead of using a designed model, a fitted model with measured response matrix is used here. The standard deviations between these two are less than 4% for the beta function and 0.6° for the phase advances. These standard deviations contain measurement errors as well as actual differences in machine conditions for the measurements. Repeated MIA measurements yield repeatability about 0.7% for the β function and 0.33° for phase advances, which reflect the random errors of MIA measurements. In addition to the phase advances between BPMs, the cumulative phase is also examined for phase variation along the ring. The repeatability for the cumulative phase is 0.24°. The phase

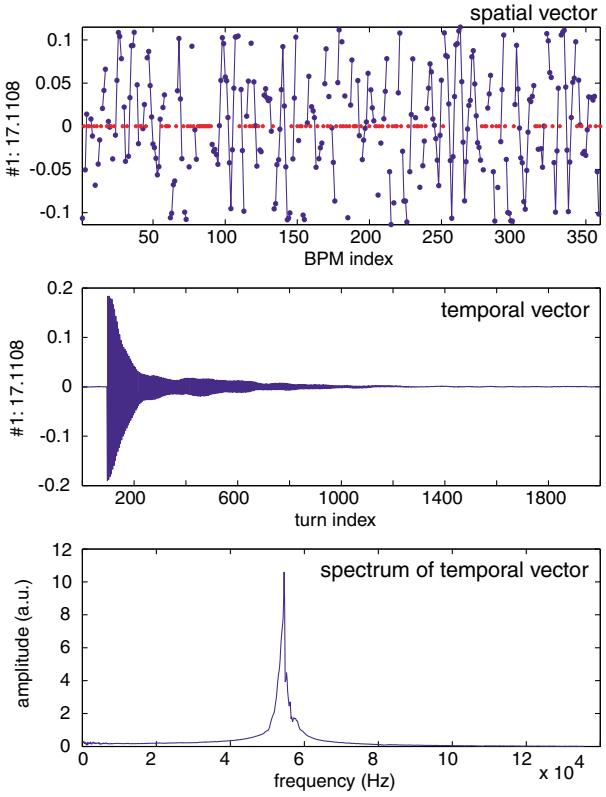

FIG. 1. (Color) The first horizontal mode with kick excitation. Blue dots are measured values and joined for consecutive BPMs. Red dots are bad BPMs. The temporal vector shows time evolution of the beam. The singular value is given after the mode number on the left labels. The spatial and temporal vectors are dimensionless and normalized to one.

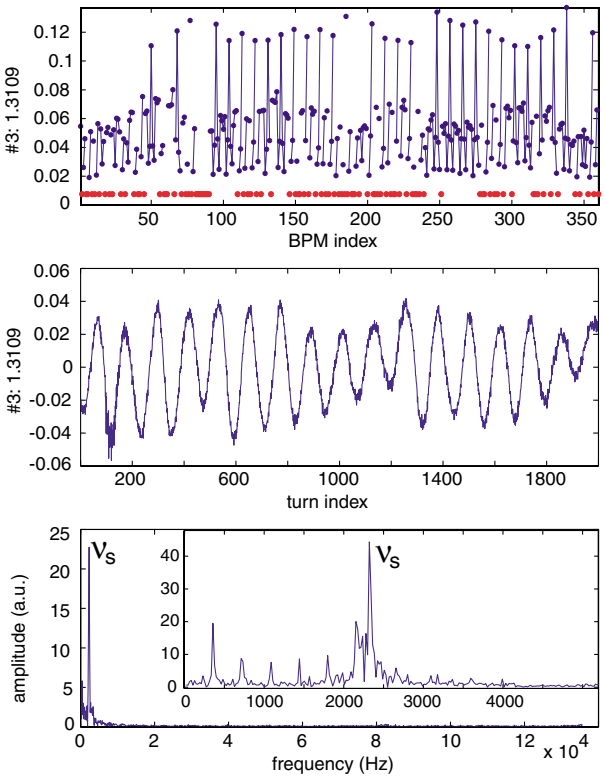

FIG. 2. (Color) The third horizontal mode: a synchrotron mode. See caption of Fig. 1 for more description.

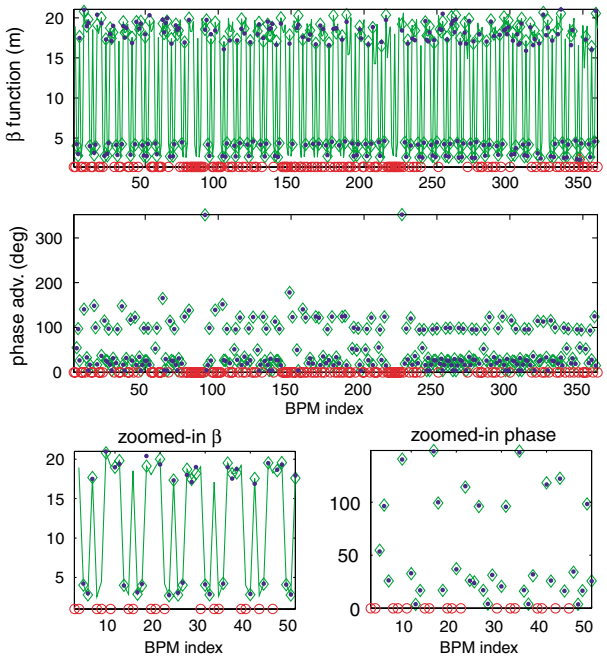

FIG. 3. (Color) Horizontal β function and phase advances between BPMs. The solid dots are MIA measurements. The solid lines are calibrated machine model. Diamonds are model values at used BPMs. Circles are malfunctioning BPMs. Figures in the third row are blowups of the above figures for the first 50 BPMs.

advance between two BPMs is the difference of two cumulative phases, thus its error is $\sqrt{2}$ larger. These errors depend on excitation amplitudes and are limited by the maximum signal achievable in the presence of strong decoherence. Furthermore, at this level, the measurements become sensitive to slight changes in machine conditions from one measurement to another. For example, the machine tunes are stable only to the level of 10^{-3}, which is 0.36° in phase.

C. Vertical measurements with resonant excitation

For the vertical plane, we use a pinger to excite betatron oscillation. The pinger can be operated with either a high-voltage pulse drive or a low-voltage cw drive. Thus we can either kick the beam or resonantly excite the beam. With kick excitation, it is similar to the horizontal plane. Because of decoherence, it turns out that resonant excitation offers a stronger signal. Figure 4 shows the first betatron mode of a resonantly excited beam. As in Fig. 1, the spatial vector gives a vertical betatron orbit. The temporal vector shows a continuously excited beam, and its Fourier spectrum shows a much narrower peak at the betatron frequency. For various reasons, it is not easy to excite a pure harmonic oscillation in the APS ring when the data were taken. Thus the oscillation amplitude has significant variation, and the spectrum shows noticeable noise around the peak. Instead of choosing a better data set, we use this one to show that our method is rather robust and works under less perfect conditions. A major difference between the horizontal and vertical planes is that there is no synchrotron mode in the vertical plane due to minute vertical dispersion.

The results for vertical β function and phase advance are shown in Fig. 5. See the description of Fig. 3 for an explanation of the figure. In this vertical case, the standard deviations between model and measurements are less than 3% for the β function and 0.5° for the phase advances. Repeatability is better than 0.6% for β function, 0.21° for phase advances between BPMs, and 0.15° for the cumulative phase (0.08° has been reached with more coherent oscillation). Occasionally, there are significant differences at a few BPMs such as those marked in the figure. BPM gains are suspected, but we have not tracked down the exact cause. Since the response-matrix measurement and the MIA measurement are carried out on different days, unexpected optics changes might also cause the differences.

For resonantly excited coherent oscillations, the harmonic-analysis method can be used to determine the phase advances. For comparison, we did such an exercise and found that the standard deviation in phase advances between the harmonic analysis and MIA methods is less than 0.2°. The repeatability of the harmonic analysis with carefully determined tune is about 0.2° for the cumulative phase, slightly worse than the MIA method. Thus, the

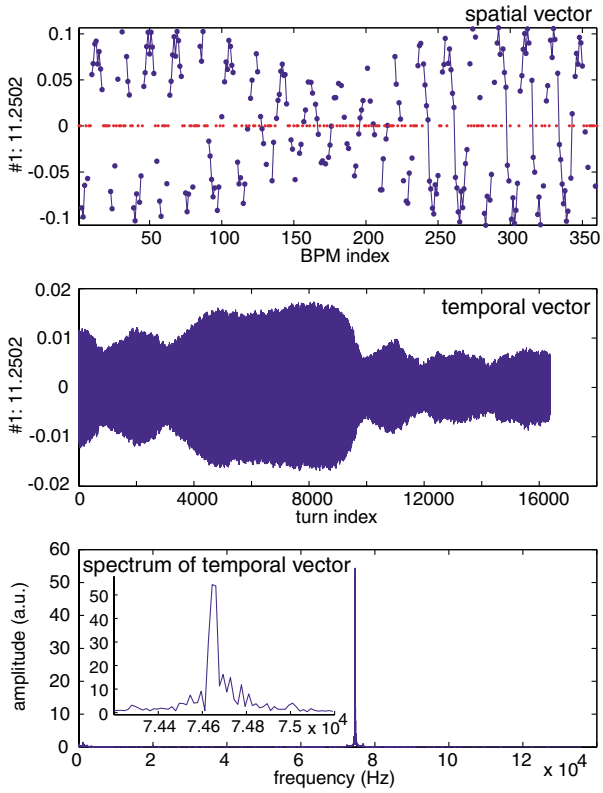

FIG. 4. (Color) The first vertical mode with resonant excitation. See caption of Fig. 1 for more description. Inset is a blowup.

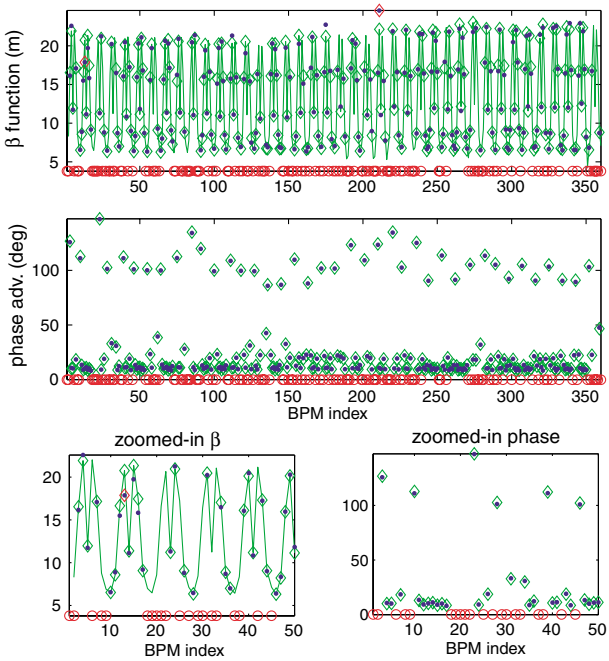

FIG. 5. (Color) Vertical β function and phase advance. See caption of Fig. 3 for more description. The red diamond indicates those with deviations larger than 3σ.

MIA method rivals the harmonic-analysis method in accuracy.

D. Measurement with excitation from instability

We showed measurements done with commonly used kick excitation and resonant excitation. In the APS storage ring, a single-bunch beam instability leads to a well-behaved bursting mode that has large periodic centroid oscillation [21]. Such a self-excited horizontal oscillation is also tested for measuring lattice functions. The first eigenmode is shown in Fig. 6.

The temporal vector shows three periods of the self-excited oscillation. The Fourier spectrum shows sharp clean betatron oscillation with two barely noticeable synchrotron sidebands. A detailed examination shows the betatron peak is heavily modulated at the bursting frequency. Again, using the spatial vector of this betatron mode, we calculated the phase advances and β function. The results agree well with the results from kick excitation shown in Fig. 3. In fact, the signal is stronger than that from the kick excitation. Comparing the results from two different bursts yields repeatability of 0.7% for the β function, 0.24° for phase advances between BPMs, and 0.18° for the cumulative phase. These are a little better than those with kick excitation.

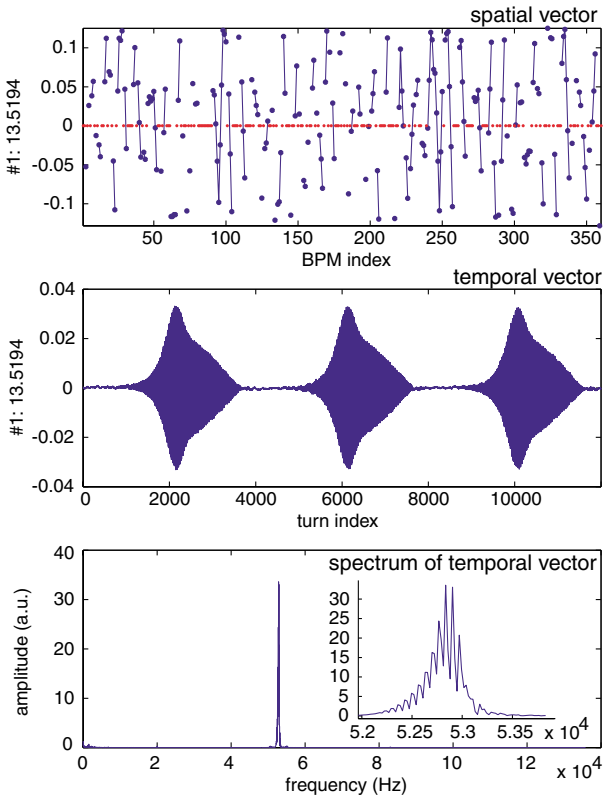

FIG. 6. (Color) Horizontal betatron mode due to instability. See caption of Fig. 1 for more description. Inset is a blowup.

This example also demonstrates one more potential benefit of our method: it is possible to extract lattice functions from beam histories taken for another purpose, e.g., instability study. Such simultaneously obtained lattice functions could help reduce uncertainty about machine conditions for the intended study, which is important especially when lattice stability is a concern.

E. Effects due to gradient error, energy offset, and wakefield

We have demonstrated a robust and accurate MIA technique to measure phase advances in a ring. It is well known that phase advance (and betatron tune of course) is sensitive to various physical effects and thus its accurate measurement provides valuable information on those effects. Here we show a few such examples to demonstrate that MIA phase-advance measurements can indeed be used to measure the local effects due to quadrupole gradient error, beam energy offset, and even wakefield. However, no detailed analysis will be given since it is not the focus of this paper.

Figure 7 shows the difference of two sets of horizontal phases measured under the same condition except that a quadrupole is changed by 0.5%. We see a clear 2° phase jump at the quadrupole location. Phase beating before and after the jump is also evident. The phase accuracy of this measurement is about 0.3° in rms.

Figure 8 shows a horizontal phase difference due to a 100-Hz rf frequency shift (about 0.1% relative energy offset). A more or less linear increase of the phase difference shows chromatic effects. The total deviation gives a good measurement of chromatic tune shift. The local chromatic phase shift could provide information on the source of the chromatic effect.

Figure 9 shows the vertical phase differences for measurements done with two different single-bunch currents at 1.1 and 4.9 mA. The total deviation measures the current detuning parameter often used for instability studies. Interesting local structures clearly exist. This is because the vertical gaps of the vacuum chambers vary significantly for different insertion devices. From the local phase-advance change with current, one can

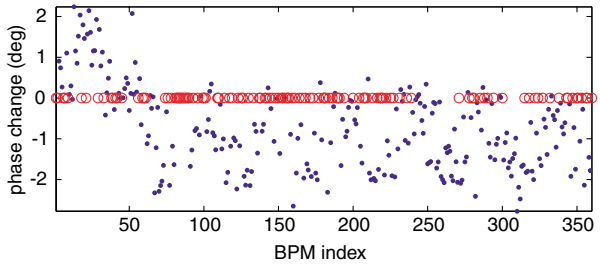

FIG. 7. (Color) Phase changes due to a 0.5% quadrupole change near the 56th BPM. The 2° phase jump and beating pattern are evident. Again the circles indicate unusable BPMs.

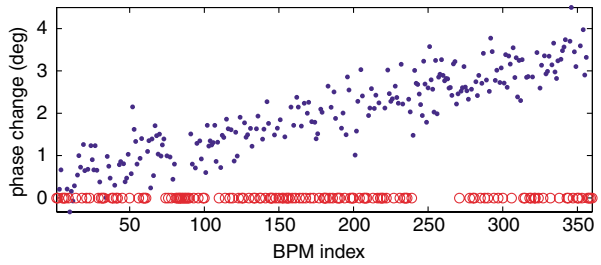

FIG. 8. (Color) Phase changes due to a 0.1% energy decrease.

estimate the local reactive impedance along the ring as done at LEP [22]. We also checked the horizontal current-dependent phase difference, which shows a much weaker wakefield effect and little structure other than a more or less linear decrease. This is because the horizontal aperture is much larger than the vertical one, and there is also not much variation along the ring.

To study the local effects in detail, it is desirable to further improve the accuracy of the phase measurement. Our measurements are limited by the achievable signal strength. In the horizontal plane, the kick excitation is limited by decoherence that damps the signal within 100 turns. In the vertical plane, the resonant excitation amplitude is currently limited to about 300 μm at low-beta BPMs and 1.2 mm at high-beta locations. In addition to improving signal strength, significant improvement may also be achieved by averaging over repeated measurements, provided that the data acquisition is fast and the machine is sufficiently stable. A preliminary test using four sets of data shows that further averaging does work. However, since our beam-history system is rather slow, we did not explore further.

F. Remarks

As discussed before, the phase-advance measurement is independent of machine model and BPM calibrations. The good agreement in phase advance supports both MIA and response-matrix measurements at the APS. On the other hand, BPM gains from response-matrix fitting are used for the β function calculation, and a fitting to the model β function is used to determine the overall scaling factor. Furthermore, our orbit response measurements and beam-history measurements use different electronic systems; thus the BPM gain calibration for one system could be different for the other. Despite these limitations in β function measurement, the result on the β function further confirms MIA analysis.

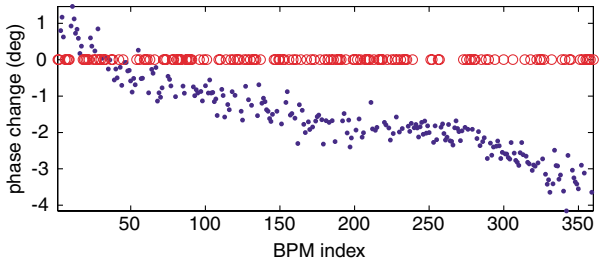

FIG. 9. (Color) Phase changes due to current-dependent wakefield.

It is desirable to be able to determine BPM gains from beam histories. Model calibration using beam histories is a promising method for determining BPM gains and transverse coupling using the same beam-history measurements. However, we have not experimentally pursued this method because the large number of malfunctioning beam histories at APS makes it rather difficult if not impossible. Because of the BPM electronic systems, APS has about twice as many BPMs good for response-matrix measurements as BPMs usable for beam-history measurements.

Dispersion is usually easy to measure from closed-orbit change with respect to rf frequency shift. Thus we have not pursued dispersion measurement using MIA. Nonetheless, a synchrotron mode such as shown in Fig. 2 can be used to measure dispersion function. For accurate measurement, one may want to resonantly excite significant synchrotron oscillations by modulating rf phase at the synchrotron frequency, for example.

The results shown in Figs. 3 and 5 have used thousands of turns of beam history. In the horizontal case, it is actually unnecessary to use this many turns, although it helps in observing low frequency modes. The betatron signal in Fig. 1 decoheres significantly in less than 100 turns. Thus using only a couple hundred turns gives equally good results.

We have used a few hundred BPMs in our measurements. However, our method works even if only a fraction of those BPMs is used. The measurement accuracy determined by repeatability tests showed no obvious M dependence for the vertical measurement. Nonetheless, for understanding a lattice, it is important to have a sufficiently large number of BPMs to determine the β function and phase advances.

IV. CONCLUSION

We have developed and experimentally demonstrated (even with a problematic broad-band BPM system) a new MIA technique to measure the phase advances of a storage ring with little coupling. Given well-calibrated BPMs, β function can be measured as well. Compared to methods based on closed-orbit measurements, our method uses beam oscillation histories that require little machine time to collect and can yield results in minutes or less, provided that a suitable broad-band BPM system is available. Compared to the harmonic analysis of orbit oscillations, which works well only for resonantly excited clean harmonic oscillations, our method applies to various types of beam excitations. Compared to model

calibration methods, our method works even when successful model calibration is prevented by an insufficient number of BPMs or lack of a good machine model. The accuracy of our method rivals other techniques. However, even though the phase-advance measurement is immune from BPM gain errors, the β function measurement does require good BPM calibration, which is a major limitation (a shortcoming compared to model calibration methods). Furthermore, while our method has yet to be extended to handle linear coupling, some of the methods mentioned above already can. Since phase advances are sensitive to various physical phenomena (we demonstrated a few of them), our simple, fast, robust, accurate, and model-independent measurement technique should be valuable to commissioning, operating, and understanding a ring. In principle this method can be adapted to linacs (by taking into account the acceleration, etc.), especially long linacs with a large number of BPMs, such as the proposed next-generation linear colliders.

ACKNOWLEDGMENTS

We would like to acknowledge help received from colleagues and the APS operation crew during this study, especially during data acquisitions. Special thanks are due to L. Emery and M. Borland for updating the data acquisition software, G. Decker for his advice on the BPM system, and K. Harkay for helpful input on instability conditions. C.W. is grateful for helpful communications with J. Irwin, Y. Yan, and Y. Cai and support from K.-J. Kim and S. Milton. This work was supported by the U.S. Department of Energy, Office of Basic Energy Sciences, under Contract No. W-31-109-ENG-38.

APPENDIX A

From Eq. (11) we know that the two betatron modes have approximately the same magnitudes with singular values $\sigma_\pm \simeq \sigma_s \equiv \sqrt{\langle J\rangle\langle\beta\rangle/2}$. Assume as well that the errors in $\xi_\pm = \sigma_\pm v_\pm$ are random and uncorrelated with about the same rms σ_ξ. Then from Eqs. (15) and (16) we have

$$\sigma_\psi = \sqrt{\left[\left(\frac{\partial\psi}{\partial\xi_+}\right)\sigma_{\xi_+}\right]^2+\left[\left(\frac{\partial\psi}{\partial\xi_-}\right)\sigma_{\xi_-}\right]^2} \simeq \sqrt{\left(\frac{\partial\psi}{\partial\xi_+}\right)^2+\left(\frac{\partial\psi}{\partial\xi_-}\right)^2}\sigma_\xi$$
$$= \frac{1}{\sqrt{\xi_+^2+\xi_-^2}}\sigma_\xi = \sqrt{\frac{\langle J\rangle}{\beta}}\sigma_\xi = \sqrt{\frac{\langle\beta\rangle}{2\beta}}\frac{\sigma_\xi}{\sigma_s} = \sqrt{\frac{\langle\beta\rangle}{2\beta}}\frac{1}{\sqrt{P}}\frac{\sigma_r}{\sigma_s}.$$

Here σ_r is the residual signal and noise magnitude, which is difficult to estimate and roughly given by the singular values beyond the betatron modes. Similarly,

$$\sigma_\beta \simeq \sqrt{\left(\frac{\partial\beta}{\partial\xi_+}\right)^2+\left(\frac{\partial\beta}{\partial\xi_-}\right)^2}\sigma_\xi = 2\beta\sigma_\psi.$$

[1] A.W. Chao and M. Tigner, *Handbook of Accelerator Physics and Engineering* (World Scientific, Singapore, 1998).

[2] F. Zimmermann, SLAC Report No. SLAC-PUB-7844, 1998.

[3] J. Borer, C. Bovet, A. Burns, and G. Morpurgo, in *Proceedings of the 3rd European Particle Accelerator Conference, Berlin, Germany, 1992* (Editions Frontières, Gif-sur-Yvette, France, 1992), p. 1082.

[4] P. Castro *et al.*, in *Proceedings of the 1993 Particle Accelerator Conference, Washington, D.C.* (IEEE, Piscataway, NJ, 1993), p. 2103.

[5] D. Sagan, R. Meller, R. Littauer, and D. Rubin, Phys. Rev. ST Accel. Beams **3**, 092801 (2000).

[6] W. J. Corbett, M. J. Lee, and V. Ziemann, in *Proceedings of the 1993 Particle Accelerator Conference, Washington, D.C.* (Ref. [4]), p. 108.

[7] W. J. Corbett, M. J. Lee, and V. Ziemann, in *International Symposium on Optics, Imaging and Instrumentation, San Diego, 1993*, SPIE Proceedings (SPIE–International Society for Optical Engineering, Bellingham, WA, 1993).

[8] J. Safranek, Nucl. Instrum. Methods Phys. Res., Sect. A **388**, 27 (1997).

[9] D. Robin, J. Safranek, G. Portmann, and H. Nishimura, in *Proceedings of the 1996 European Particle Accelerator Conference, Sitges, Spain* (IOP, Bristol, UK, 1996), p. 971.

[10] V. Sajaev and L. Emery, in *Proceedings of the 2002 European Particle Accelerator Conference, Paris, France* (EPS-IGA, Geneva, 2002), p. 742.

[11] J. Irwin and Y.T. Yan, in *Proceedings of the 2000 European Particle Accelerator Conference, Vienna, Austria* (EPS-IGA, Geneva, 2000), p. 151.

[12] Y. Cai, J. Irwin, M. Sullivan, and Y.T. Yan, in *Proceedings of the 2001 Particle Accelerator Conference, Chicago* (IEEE, Piscataway, NJ, 2001), p. 3555.

[13] Y. Yan, Y. Cai, J. Irwin, and M. Sullivan, SLAC Report No. SLAC-PUB-9368, 2002.

[14] J. Irwin *et al.*, Phys. Rev. Lett. **82**, 1684 (1999).

[15] Chun-xi Wang, Ph.D. thesis, Stanford University, 1999; also SLAC Report No. SLAC-R-547, 2003.

[16] R. Gnanadesikan, *Methods for Statistical Data Analysis of Multivariate Observations* (Wiley, New York, 1997), 2nd ed.

[17] T.W. Anderson, *An Introduction to Multivariate Statistical Analysis* (Wiley, New York, 1984), 2nd ed.

[18] Gene H. Golub and Charles F. Van Loan, *Matrix Computations* (The Johns Hopkins University Press, Baltimore, 1996), 3rd ed., p. 451.

[19] Chun-xi Wang, Michael Borland, Vadim Sajaev, and Kwang-Je Kim, in *Proceedings of the 2001 Particle Accelerator Conference, Chicago* (Ref. [12]), p. 1355.

[20] Chun-xi Wang, in Proceedings of the 2003 Particle Accelerator Conference, Portland (to be published).

[21] K. Harkay, Z. Huang, E. Lessner, and B. Yang, in *Proceedings of the 2001 Particle Accelerator Conference, Chicago* (Ref. [12]), p. 1915.

[22] D. Brandt *et al.*, in *Proceedings of the 1995 Particle Accelerator Conference, Dallas* (IEEE, Piscataway, NJ, 1995), p. 570.